

Pulsed Nuclear Magnetic Resonance of Na²³ in Rapidly Rotated NaCl†

A. C. CUNNINGHAM* AND S. M. DAY

Department of Physics, University of Arkansas, Fayetteville, Arkansas

(Received 25 January 1966; revised manuscript received 5 August 1966)

High-speed sample-rotation studies of nuclear relaxation processes of Na²³ in powdered NaCl are presented. A qualitative theory of the free-induction-decay shape under sample rotation is compared with experiment. The principal effects of sample rotation on the central line component for NaCl occur at rotation frequencies below the root-mean-square second moment in frequency units, in agreement with previous theories. First-order quadrupolar broadening can be eliminated provided sufficiently high rotation rates can be achieved.

INTRODUCTION

NUCLEAR magnetic resonance (NMR) is a useful tool for the study of the electric and magnetic environment of nuclei within a solid. However, unlike motionally narrowed liquids, the NMR absorption line shape of solids is usually determined by dipole-dipole interactions. This dipolar broadening often obscures the more interesting features of the lineshape thus limiting the usefulness of nuclear resonance.

By rotating a solid sample at high angular velocities, it is possible to "motionally narrow" the absorption line. That is, the effect of dipole-dipole interactions can be greatly reduced by sample rotation. In addition, some spin-lattice relaxation processes can be affected by sample rotation.

The effect of sample rotation on the free-induction-decay process and spin-lattice relaxation time for Na²³ in powdered NaCl are reported along with a discussion of the relaxation processes.

THEORY

A detailed theory of the effect of high-speed sample rotation on the nuclear resonance absorption lineshape of a nuclear pair has been given by Drietlein and Kessemeier.¹ More recently, Clough and Gray,² and Kessemeier³ have investigated sample rotation effects on nuclear magnetic relaxation processes using a stochastic approach in the theory. In this section a more qualitative approach is taken resorting to a phenomenological presentation.

The principal contributions to the resonance line-width of a solid at room temperature are the dipole-dipole interaction and the interaction of the nuclear electric quadrupole moments with the crystalline electric field gradients.

The interaction Hamiltonian for a spin *i* may be written as a sum of a magnetic dipolar term \mathcal{H}_i^m and

an electric quadrupolar term \mathcal{H}_i^Q . Using operators associated with the Zeeman frame, \mathcal{H}_i^m is given by⁴

$$\mathcal{H}_i^m = \sum_{j \neq i} \hbar^2 \gamma_i \gamma_j (\mathbf{r}_{ij})^{-3} \times [A_{ij} + B_{ij} + C_{ij} + D_{ij} + E_{ij} + F_{ij}], \quad (1)$$

with

$$\begin{aligned} A_{ij} &= (1 - 3 \cos^2 \theta_{ij}) I_{zi} S_{zj}, \\ B_{ij} &= -\frac{1}{4} (1 - 3 \cos^2 \theta_{ij}) (I_{+i} S_{-j} + I_{-i} S_{+j}), \\ C_{ij} &= D_{ij}^* = -\frac{3}{4} \sin 2\theta_{ij} e^{-i\phi_{ij}} (I_{zi} S_{+j} + I_{+i} S_{zj}), \\ E_{ij} &= F_{ij}^* = -\frac{3}{4} \sin 2\theta_{ij} e^{-2i\phi_{ij}} S_{+j} I_{+i}, \end{aligned}$$

where θ_{ij} and ϕ_{ij} are the polar and azimuthal angles of the internuclear vector \mathbf{r}_{ij} . Only the first two terms will be retained leaving the truncated Hamiltonian. The neglected terms would only be important if the sample rotation rate were of the order of the Larmor frequency.

Again using operators associated with the Zeeman frame, but expressing the electric field gradients in the crystalline principal axis system, \mathcal{H}_i^Q is given by⁵ [see Appendix, Eq. (A13)]

$$\begin{aligned} \mathcal{H}_i^Q &= K \{ V_{zzi}^P [\frac{1}{2} (3I_{zi}^2 - I_i^2) (3 \cos^2 \theta - 1) \\ &\quad + \frac{3}{4} (I_{+i} I_{zi} + I_{zi} I_{+i}) \sin 2\theta e^{-i\psi} \\ &\quad + \frac{3}{4} I_{+i}^2 \sin^2 \theta e^{-2i\psi} + \text{c.c.}] \\ &\quad + (V_{xxi}^P - V_{yyi}^P) [-\frac{1}{2} (3I_{zi}^2 - I_i^2) \sin^2 \theta \cos 2\phi \\ &\quad + \frac{1}{2} (I_{zi} I_{+i} + I_{+i} I_{zi}) (i \sin \theta \sin 2\phi e^{-i\psi} \\ &\quad + \frac{1}{2} \sin 2\theta \cos 2\phi e^{-i\psi}) \\ &\quad - \frac{1}{2} I_{+i}^2 (\frac{1}{2} (1 + \cos^2 \theta) \cos 2\phi e^{-2i\psi} \\ &\quad + i \cos \theta \sin 2\phi e^{-2i\psi}) + \text{c.c.}] \}, \quad (2) \end{aligned}$$

with

$$K = \frac{eQ}{4I(2I-1)},$$

and where θ , ϕ , and ψ are the Eulerian angles of the crystalline principal axes in the Zeeman frame.

If the sample is rotated about a direction inclined at an angle Θ with the external magnetic field at rota-

† Supported by the National Science Foundation.

* Present address: Martin Company, Denver, Colorado.

¹ J. Drietlein and H. Kessemeier, Phys. Rev. **123**, 835 (1961).

² S. Clough and K. W. Gray, Proc. Phys. Soc. (London) **79**, 457 (1962).

³ H. Kessemeier, thesis, Washington University, 1964 (unpublished).

⁴ J. H. Van Vleck, Phys. Rev. **74**, 1168 (1948).

⁵ C. P. Slichter, *Principles of Magnetic Resonance* (Harper & Row, New York, 1963), p. 172.

tional velocity Ω , the interaction Hamiltonians become time-dependent. (See Appendix for transformation equations). The truncated dipolar Hamiltonian becomes

$$\mathcal{H}_i^{m'}(t) = \sum_{j \neq i} \gamma_i \gamma_j \hbar^2 (r_{ij})^{-3} [A_{ij}(t) + B_{ij}(t)], \quad (3)$$

with

$$\begin{aligned} A_{ij}(t) + B_{ij}(t) = & -\frac{1}{2} [I_{zi} S_{zj} - \frac{1}{4} (I_{+i} S_{-j} + I_{-i} S_{+j}) \\ & [(1-3 \cos^2 \Theta)(1-3 \cos^2 \theta_{ij}') \\ & + 3 \sin 2\Theta \sin 2\theta_{ij}' \cos(\Omega t + \phi_{ij}') \\ & + 3 \sin^2 \Theta \sin^2 \theta_{ij}' \cos 2(\Omega t + \phi_{ij}')], \end{aligned}$$

where θ_{ij}' and ϕ_{ij}' are the polar and azimuthal angles of the internuclear vector \mathbf{r}_{ij} at $t=0$.

Under sample rotation, the quadrupolar term diagonal in the Zeeman representation is given by

$$\begin{aligned} \mathcal{H}_i^{Q'}(t) = & \frac{1}{4} K (3I_{zi}^2 - I_i^2) \{ V_{zzi}^P [(1-3 \cos^2 \Theta)(1-3 \cos^2 \theta) \\ & + 3 \sin 2\Theta \sin 2\theta \cos(\Omega t + \psi) \\ & + 3 \sin^2 \Theta \sin^2 \theta \cos 2(\Omega t + \psi)] \\ & + (V_{xxi}^P - V_{yyi}^P) [(1-3 \cos^2 \Theta)(1-3 \cos^2 \theta) \\ & + \sin 2\Theta (\frac{1}{2} \sin 2\theta \cos \phi \cos(\Omega t + \psi) \\ & + \sin \theta \sin 2\phi \sin(\Omega t + \psi) \\ & - \sin^2 \Theta (\frac{1}{2} (1 + \cos^2 \theta) \cos 2\phi \cos 2(\Omega t + \psi) \\ & + \cos \theta \sin 2\phi \sin 2(\Omega t + \psi))] \}. \quad (4) \end{aligned}$$

If the period of rotation (Ω^{-1}) is short compared to the lifetime of a spin state, so that a given nucleus has ample time to "see" all orientations, the time-dependent terms in the Hamiltonian can be averaged to zero. In this case the interaction Hamiltonians become

$$\begin{aligned} \langle \mathcal{H}_i^{m'}(t) \rangle = & \sum_{j \neq i} \gamma_i \gamma_j \hbar^2 (r_{ij})^{-3} (-\frac{1}{2}) [I_{zi} S_{zj} - \frac{1}{4} \\ & \times (I_{+i} S_{-j} + I_{-i} S_{+j})] (1-3 \cos^2 \Theta)(1-3 \cos^2 \theta_{ij}'), \quad (5) \end{aligned}$$

and

$$\langle \mathcal{H}_i^{Q'}(t) \rangle = \frac{1}{4} K (3I_{zi}^2 - I_i^2) (V_{zzi}^P + V_{xxi}^P - V_{yyi}^P) \times (1-3 \cos^2 \Theta)(1-3 \cos^2 \theta). \quad (6)$$

In both equations (5) and (6), the time-averaged Hamiltonians can be made to vanish if Θ is chosen such that $(1-3 \cos^2 \Theta_c) = 0$. It is interesting to note that in the quadrupolar case no reference is made to the symmetry of the field gradient. The residual linewidth is due to either isotropic interactions or interactions which have a different angular dependence from those discussed above.

A second case of interest occurs when the rotation axis is perpendicular to the applied magnetic field ($\Theta = 90^\circ$). The magnetic dipolar Hamiltonian under rotation becomes $\frac{1}{2}$ of that for the static case and thus one could expect the resonance line to be narrowed by a factor of 2 for pure dipolar interaction. Likewise if the sample has electric field gradients with cylindrical symmetry ($V_{xxi}^P = V_{yyi}^P$), then $\mathcal{H}_i^{Q'}$ is reduced by a factor of two at $\Theta = 90^\circ$.

Line-Shape Effects

It has been observed experimentally by Andrew, Bradbury, and Eades⁶ that the resonance spectrum of Na^{23} in a rotated crystal of NaCl for $\Theta = \Theta_c$ consists of a narrowed central portion and side spectra of decreasing amplitude spaced at integral multiples of the rotation rate. The formation of the side spectra is attributed to the time-dependent terms in the Hamiltonians of equations (3) and (4). Since the free-induction-decay curve is the Fourier transform of the resonance spectrum, some elementary considerations of the spectral lineshape should lead to a qualitative measure of the free-induction-decay structure.

For simplicity, it is assumed that the central portion and side spectra have the same general lineshape $f(\omega)$, where the first side spectra are reduced in amplitude by the factor $\frac{1}{2}a < 1$, the second reduced by the factor $\frac{1}{2}b < \frac{1}{2}a$, and all others are negligible. Assuming the side spectra to be sufficiently removed from the center portion so there is no overlap, the Fourier transform of the sum of the lines will equal the sum of the Fourier transforms of each line taken separately. We also assume the center portion and side spectra to be independent, i.e., there is no coupling between them. Shifting the center frequency ω_0 to the origin, the free-induction decay $G(t)$ is then

$$\begin{aligned} G(t) = & \int_{-\infty}^{\infty} [f(\omega) + \frac{1}{2}a f(\omega + \Omega) + \frac{1}{2}a f(\omega - \Omega) \\ & + \frac{1}{2}b f(\omega + 2\Omega) + \frac{1}{2}b f(\omega - 2\Omega)] e^{i\omega t} d\omega. \quad (7) \end{aligned}$$

Denoting as $f(t)$ the Fourier transform of the center portion $f(\omega)$, we have

$$G(t) = f(t) [1 + a \cos \Omega t + b \cos 2\Omega t]. \quad (8)$$

Thus the free-induction-decay curve consists of "wiggles" called "spinning beats" of frequency Ω and 2Ω , with initial amplitude a and b , respectively, superimposed on the Fourier transform of the central line, $f(t)$.

Note that for $\Theta = 90^\circ$, the $\cos \Omega t$ terms in the Hamiltonian [Eqs. (3) and (4)] are absent; thus only side spectra spaced at even multiples of the rotation rate Ω are present. In this case, the spinning beats superimposed on the decay curve $f(t)$ have frequency 2Ω only, and are smaller in initial amplitude than for $\Theta = \Theta_c$ since $b < a$.

The second moment of the resonance line is invariant under sample rotation and is given by⁷

$$M_2 = - \left(\frac{d^2 G(t)}{dt^2} \right)_{t=0} / G(0). \quad (9)$$

⁶ E. R. Andrew, A. Bradbury, and R. G. Eades, *Nature* **182**, 1659 (1958).

⁷ A. Abragam, *The Principles of Nuclear Magnetism* (Oxford University Press, London, 1961), p. 110.

From Eqs. (8) and (9), the second moment under sample rotation becomes

$$M_2 = \frac{a+4b}{1+a+b} \Omega^2 + m_2(\Omega), \quad (10)$$

where $m_2(\Omega)$ is the second moment of the central component only. It should be pointed out that a and b are also functions of Ω and their form depends on the interactions present in the sample. However, in the limit of $\Omega \rightarrow \infty$, the first term in Eq. (10) should approach a constant value. The difference between this constant and M_2 gives the second moment of the central line component.

The fourth moment of the absorption line in terms of the free induction decay function is given by

$$M_4 = \left(\frac{d^4 G(t)}{dt^4} \right)_{t=0} / G(0). \quad (11)$$

From Eqs. (8) and (11), M_4 becomes

$$M_4 = \frac{a+16b}{1+a+b} \Omega^4 + 6m_2 \frac{a+4b}{1+a+b} \Omega^2 + m_4, \quad (12)$$

where m_4 is the fourth moment of the central line component under rotation. M_4 is not invariant under sample rotation, thereby making it difficult to discuss the effect of rotational velocity on m_4 .

Impurity Relaxed Solids

In an impurity relaxed solid, energy is transferred from one nucleus to another via energy-conserving mutual spin-flips as described by the Hamiltonian⁸

$$\mathcal{H}_{ij} = \frac{1}{4} \gamma^2 \hbar^2 (r_{ij})^{-3} [I_{+i} I_{-j} + I_{-i} I_{+j}] (3 \cos^2 \theta_{ij} - 1).$$

A few nuclei interact with neighboring paramagnetic impurities via interactions which do not conserve energy, such as those described by the Hamiltonian

$$\mathcal{H}_{is} = -\frac{3}{4} \gamma \gamma_s \hbar^2 (r_{is})^{-3} [I_{\pm i} S_z] \sin 2\theta_{is} e^{\mp i\phi_{is}}.$$

In a typical solid at room temperature, the former interaction is much weaker than the latter, and thus the rate of energy transfer from the spin system to the lattice is governed solely by the diffusion rate.^{9,10} This is called diffusion-limited relaxation. Since T_1 is then solely governed by the interaction proportional to $(3 \cos^2 \theta - 1)^2$, for this case, we should expect T_1 to increase dramatically as the sample is rotated at $\Theta = \Theta_c$. At the angle $\Theta = 90^\circ$, we have seen that the interaction giving rise to diffusion is reduced by $\frac{1}{2}$, thus T_1 should also increase at this angle.

⁸ N. Bloembergen, *Physica* **15**, 386 (1949).

⁹ S. M. Day, E. Otsuka, and B. Josephson, Jr., *Phys. Rev.* **137**, A108 (1965).

¹⁰ H. Rorschach, *Physica* **30**, 38 (1964).

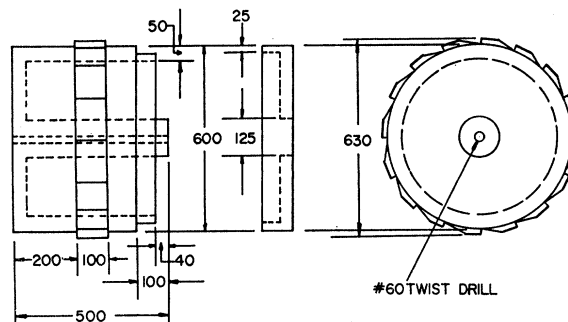


FIG. 1. Nylon sample rotor filled with powdered NaCl capable of rotation rates of over 3000 Hz. All dimensions are in mils.

Quadrupole Relaxed Solids

The transition probability for a spin to transfer energy to the lattice via the electric quadrupole interaction should not be influenced by sample rotation unless the rotational frequency approaches the Larmor frequency. However, T_1 could be affected by the decoupling of the spins due to sample rotation if T_2 became the order of T_1 . In this case, the spin temperature treatment of Hebel and Slichter¹¹ would not be valid and the approach to equilibrium of the spin system to the lattice would not be given by a single time constant. In no experiment reported to date has T_2 approached T_1 under sample rotation, thus it would be expected that T_1 due to quadrupolar relaxation, should be invariant under sample rotation.

EXPERIMENTAL APPARATUS AND PROCEDURE

The pulsed free-induction spectrometer was conventional in design. A continuous rf signal was gated, amplified, and sent to the sample coil which served as both the transmitter and receiver coil. The transmitter was capable of providing a 90° pulse for Na²³ in less than 15 μ sec. The receiver recovered completely in 10 μ sec following a pulse. All data were taken using 10.5 MHz. The free-induction-decay curves were photographed from the oscilloscope. A number of curves were superposed and a smooth curve drawn. Because of the nonlinear characteristics of the detector circuit, it was necessary to make a diode correction.

The powdered NaCl sample was contained in a rotor shown in Fig. 1. The cylindrical axis of the rotor was colinear with the cylindrical axis of the sample coil. The rotor was machined from nylon and the end cap was sealed to the main body with Kodak 910 contact adhesive. Many rotors were made of various sizes and shapes and it was found that rotors with a diameter-to-length ratio larger than 1 were most stable. Various materials were tried for the rotor. Teflon was found to be a poor material because it flowed outward at prolonged spinning rates above 1.5 kHz. Lucite worked well up to 2.5 kHz, but tended to explode above this

¹¹ L. C. Hebel and C. P. Slichter, *Phys. Rev.* **113**, 1504 (1959).

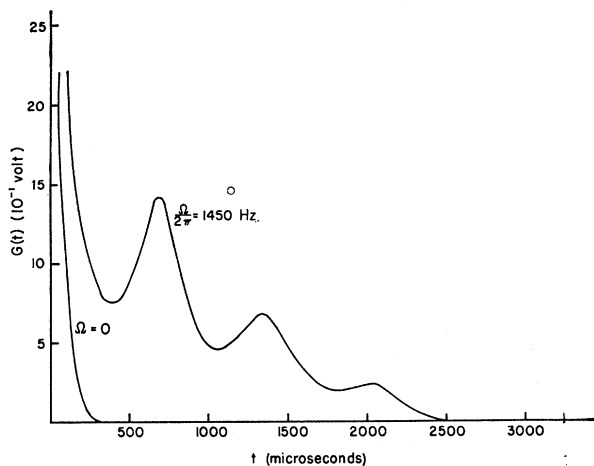


Fig. 2. Free-induction-decay curve of Na^{23} in powdered NaCl for $\Omega/2\pi=0$ and 1450 Hz with $\Theta=\Theta_c=\cos^{-1}(1/\sqrt{3})$.

rate. Nylon proved to be the best material as no observable distortion occurred and no samples exploded. The rotor was driven by a single air jet. The gas pressure was regulated between 0 and 80 psi. To obtain 2.7 kHz a pressure of 60 psi was used.

Considerable care was taken in setting the magnetic field and the pulse duration. It was found that the field had to be set within 0.25 G of the resonant value. The setting of the angle Θ between the rotation direction and the magnetic field was within 1° of the desired value.

RESULTS

Shown in Fig. 2 and 3 are the free-induction-decay curves at $\Theta = \Theta_c$ for $\Omega/2\pi=1450$, and 2400 Hz, respectively. Shown also for comparison is the free-induction-decay curve for $\Omega=0$. For $\Theta=90^\circ$, the free-induction-decay curves for $\Omega/2\pi=0$, 1100, 2000, and 2700 Hz are shown in Fig. 4. Shown in Fig. 5 are calculated curves of $f(t)$ for $\Omega/2\pi=1450$, 2000, and 2400 Hz. These curves represent the Fourier transform of the center line of the resonance spectrum in the absence of side spectra. They were obtained by curve fitting from the equation

$$f(t) = G(t)[1 + a \cos \Omega t + b \cos 2\Omega t]^{-1},$$

using various trial values of a and b until a smooth curve was obtained, where $G(t)$ is the free-induction-decay curve for $\Omega/2\pi=1450$, 2000, and 2450 Hz.

The growth of the magnetization to its equilibrium value was plotted by measuring the amplitude of the free-induction decay from a 90° pulse at 10-sec intervals up to 120 sec after an initial 90° pulse. The average value of many pictures taken at each 10-sec interval was diode-corrected and plotted. A smooth curve through these points represents the growth curve with characteristic time T_1 . Measurements were made at $\Theta = \Theta_c$ for $\Omega/2\pi=0$ and 2000 Hz. For $\Omega=0$, T_1 was 15 ± 2 sec, while for $\Omega/2\pi=2000$ Hz, T_1 was 20 ± 3 sec.

No significant departure from a single exponential curve was observed.

DISCUSSION OF RESULTS

From Fig. 2 and 3, it is clear that the spin-spin interaction is severely weakened by sample rotation at $\Theta = \Theta_c$. In addition, the spinning beats have the correct frequency. From Fig. 5 the most significant narrowing of the central line occurs for rotation rates below $\Omega/2\pi = 1400$ Hz and does not change significantly up to $\Omega/2\pi = 2400$ Hz. That is, a plateau appears to occur in the linewidth as a function of rotation rate. The theoretical root-mean-square second moment of NaCl due to dipolar interactions is about 800 Hz. Thus, the rotation frequencies employed in the experiment should have been high enough to essentially eliminate dipolar broadening. However, the sample employed in the experiment was a powder, which means significant quadrupolar broadening was present. This was confirmed by comparing the free-induction-decay signal of a single crystal of NaCl to that of the unrotated powder. Consequently, the resonance line may have been too broad for the rotational frequencies employed to effectively motionally narrow the entire resonance line.

Using the values of a and b from Fig. 5, the values of $(a+4b/1+a+b)(\Omega/2\pi)^2$ [Eq. (10)] are 0.8×10^6 , 1.5×10^6 and 1.6×10^6 Hz^2 at $\Omega/2\pi=1400$, 2000, and 2400 Hz, respectively. The contribution to the total second moment M_2 due to the sidebands appears to have almost leveled off at $\Omega/2\pi=2400$ Hz. Making the uncertain assumption that the second moment associated with the side bands at $\Omega/2\pi=2400$ Hz is equal to the second moment of the entire line, qualitative information can be obtained for the effect of rotation on the fourth moment M_4 . By neglecting m_4 in equation (12) and using the values of a and b given in Fig. 5, the values of M_4 are 8×10^{12} , 15×10^{12} , and 21×10^{12} Hz^4

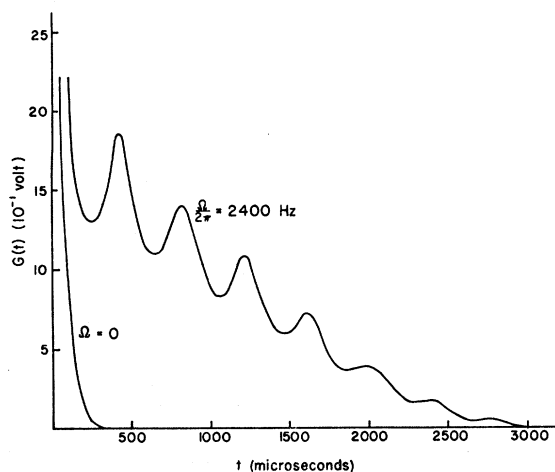


Fig. 3. Free-induction-decay curve of Na^{23} in powdered NaCl for $\Omega/2\pi=0$ and 2400 Hz with $\Theta=\Theta_c=\cos^{-1}(1/\sqrt{3})$.

at $\Omega/2\pi=1400$, 2000, and 2400 Hz, respectively. This shows rather dramatically that the effect of sample rotation is to make the resonance line become Lorentzian as Ω is increased. Furthermore, the central line component becomes Lorentzian as Ω is increased as is evident from the form of $f(t)$ in Fig. 5. In addition the intensity of the central component increases as the intensity of the side bands decrease with an increase in Ω . This is not shown in Fig. 5 as the curves were normalized to the same initial height to better show the change in shape with rotation rate. However, it is clear from Eq. (8) that since $G(0)$ is independent of Ω , $f(0)$ must increase as $(1+a+b)$ decreases.

No satisfactory explanation exists for the increase of T_1 for the rotated sample except possibly that the relaxation may be due to electronic paramagnetic impurities for the static sample and due to the electric quadrupole interaction for the rotated sample. Certainly T_2 is very small compared to T_1 , so that the spin temperature concept should be valid.

CONCLUSIONS

The effect of sample rotation on the free-induction-decay curves of Na²³ in NaCl can be explained qualitatively. At rotation frequencies several times the unrotated linewidth, further increase in the rotation rate has little effect on the second moment of the central line. Thus there is a broadening interaction which is essentially rotationally invariant in powdered NaCl. It has been shown that electric quadrupole broadening can be diminished by sample rotation regardless of symmetry provided the sample rotation rate can be made large enough.

Finally, by refining the experimental procedure and increasing the rotation rate, it should be possible to study rotationally invariant interactions in solids normally obscured by dipolar and quadrupolar interactions.

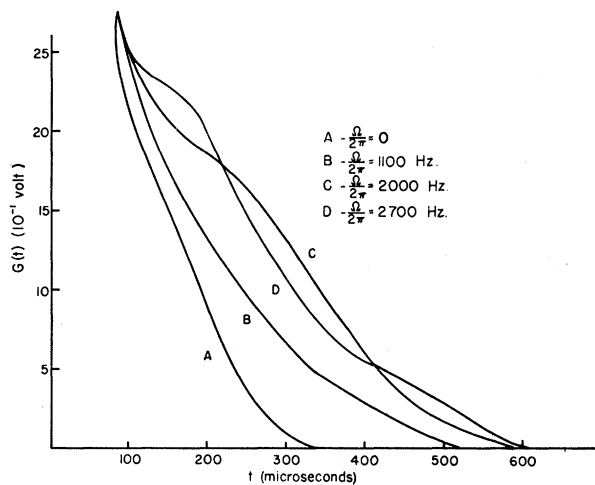


FIG. 4. Free-induction-decay curves of Na²³ in powdered NaCl for $\Omega/2\pi=0$, 1100, 2000, and 2700 Hz with $\Theta=90^\circ$.

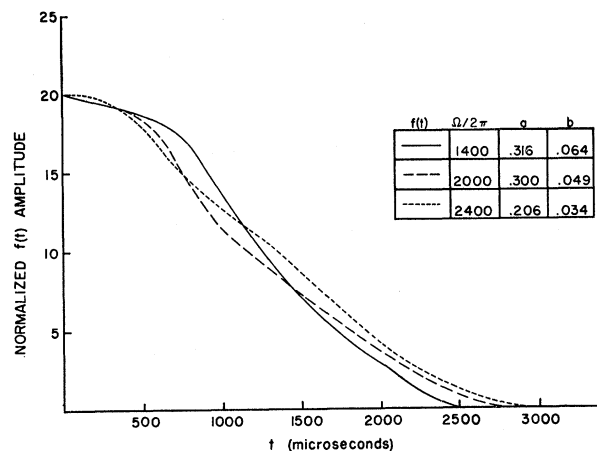


FIG. 5. Calculated free-induction-decay curve $f(t)$ of central line for $\Omega/2\pi=1450$, 2000, and 2600 Hz with $\Theta=\Theta_c=\cos^{-1}(1/\sqrt{3})$.

ACKNOWLEDGMENTS

The authors wish to thank Dr. Horst Kessemeier for several helpful discussions and for kindly giving us a copy of his thesis. We are also indebted to David Sloop and Darrell Hutchins for assistance in conducting the experiment.

APPENDIX

Transformation of Dipolar Hamiltonian

The time dependence of the internuclear vector \mathbf{r}_{ij} is needed. We perform a coordinate transformation from the laboratory frame $(\theta(t), \phi(t))$ in which the axis of rotation is along the polar axis z' . The following transformation is employed:

$$\begin{aligned} x &= x' \cos\Theta - z' \sin\Theta, \\ y &= y', \\ z &= z' \cos\Theta + x' \sin\Theta. \end{aligned} \quad (\text{A1})$$

The internuclear unit vector then becomes, in the unprimed system,

$$\hat{r} = \hat{x} \sin\theta(t) \cos\phi(t) + \hat{y} \sin\theta(t) \sin\phi(t) + \hat{z} \cos\theta(t), \quad (\text{A2})$$

and in the primed system,

$$\hat{r} = \hat{x}' \sin\theta' \cos(\Omega t + \phi') + \hat{y}' \sin\theta' \sin(\Omega t + \phi') + \hat{z}' \cos\theta'. \quad (\text{A3})$$

From (A1) and (A2), \hat{r} becomes

$$\begin{aligned} \hat{r} &= \hat{x} [\cos\Theta \sin\theta' \cos(\Omega t + \phi') - \sin\Theta \cos\theta_j \\ &\quad + \hat{y} \sin\theta' \sin(\Omega t + \phi') \\ &\quad + \hat{z} [\cos\Theta \cos\theta' + \sin\Theta \sin\theta' \cos(\Omega t + \phi')]. \end{aligned} \quad (\text{A4})$$

Using (A2) and (A4), the appropriate angular factors are easily obtained:

$$1 - 3 \cos^2\theta(t) = 1 - 3[\hat{r} \cdot \hat{z}]^2, \quad (\text{A5})$$

$$\sin\theta(t) \cos\theta(t) e^{\pm i\phi(t)} = [\hat{r} \cdot \hat{z}][\hat{r} \cdot (\hat{x} \pm i\hat{y})], \quad (\text{A6})$$

and

$$\sin^2\theta(t)e^{\pm 2i\phi(t)} = [\hat{r} \cdot (\hat{x} \pm i\hat{y})]^2. \quad (\text{A7})$$

Transformation of the Electric Quadrupolar Hamiltonian

In terms of the principal axes X, Y, Z of the tensor which describes the electric field gradient, the quadrupolar Hamiltonian may be written as

$$\mathcal{H}^Q = K \{ V_{zz}^P [3(I_z^P)^2 - I^2] + (V_{xx}^P - V_{yy}^P) \times [(I_x^P)^2 - (I_y^P)^2] \}; \quad (\text{A8})$$

$$K = \frac{eQ}{4I(2I-1)}.$$

The operators in the principal axis system (X, Y, Z) can be written in terms of the system in which the axis of rotation is the polar axis (x', y', z') as follows:

$$I_z^P = \cos\theta I_z' + \frac{1}{2}e^{i\psi} \sin\theta I_- + \frac{1}{2}e^{-i\psi} \sin\theta I_+, \quad (\text{A9})$$

and

$$I_{\pm}^P = -i \sin\theta e^{i\psi} I_{\pm}' + ie^{i\psi} [\cos^2(\theta/2) e^{-i\psi} I_{\pm}' + \sin^2(\theta/2) e^{i\psi} I_{\mp}']. \quad (\text{A10})$$

Here θ, ϕ, ψ are the Eulerian angles. (See Goldstein¹² for figure.) For sample rotation at angular velocity $\Omega, \psi = \Omega t + \psi'$. Using the transformation (A1) between the x', y', z' coordinates and the system (x, y, z) in which the external field H_0 is along the polar axis, the operators in the principal-axis system become

$$I_z^P = I_z [\cos\Theta \cos\theta + \sin\Theta \sin\theta \sin\psi] + I_+ [-\frac{1}{2} \sin\Theta \cos\theta - \frac{1}{2}i \sin\theta (\cos\psi + i \cos\Theta \sin\psi)] + I_- [-\frac{1}{2} \sin\Theta \cos\theta + \frac{1}{2}i \sin\theta (\cos\psi - i \cos\Theta \sin\psi)], \quad (\text{A11})$$

and

$$I_{\pm}^P = I_{\pm} e^{i\psi} \{ -i \cos\Theta \sin\theta + \sin\Theta [\cos^2(\theta/2) e^{i\psi} \sin^2(\theta/2) e^{-i\psi}] \} + I_+ e^{i\psi} [\frac{1}{2}i \sin\Theta \sin\theta + \frac{1}{2} \cos^2(\theta/2) (1 + \cos\Theta) e^{i\psi} - \frac{1}{2} \sin^2(\theta/2) (1 - \cos\Theta) e^{-i\psi}] + I_- e^{i\psi} [\frac{1}{2}i \sin\Theta \sin\theta - \frac{1}{2} \cos^2(\theta/2) (1 - \cos\Theta) e^{i\psi} + \frac{1}{2} \sin^2(\theta/2) (1 + \cos\Theta) e^{-i\psi}]. \quad (\text{A12})$$

Recalling that $I_x^2 - I_y^2 = \frac{1}{2}[I_+^2 + I_-^2]$ and using (A11) and (A12), \mathcal{H}^Q becomes

$$\mathcal{H}^Q = \frac{K}{4} V_{zz}^P \{ (3I_z^2 - I^2) [(1 - 3 \cos^2\Theta)(1 - 3 \cos^2\theta) + 3 \sin 2\Theta \sin 2\theta \cos\psi + 3 \sin^2\Theta \sin^2\theta \cos 2\psi] - 3(I_+ I_z + I_z I_+) [\sin 2\Theta (1 - \frac{3}{2} \sin^2\theta) - \cos 2\Theta \sin 2\theta \cos\psi + i \cos\Theta \sin 2\theta \sin\psi - \frac{1}{2} \sin 2\Theta \sin^2\theta \cos 2\psi + i \sin\Theta \sin^2\theta \sin 2\psi] + 3I_+^2 [\sin^2\Theta (1 - \frac{3}{2} \sin^2\theta) - \frac{1}{2} \sin 2\Theta \sin 2\theta \cos\psi + i \sin\Theta \sin 2\theta \sin\psi + \frac{1}{2} (1 + \cos^2\Theta) \sin^2\theta \cos 2\psi - i \cos\Theta \sin^2\theta \sin 2\psi] + \text{c.c.} \} + \frac{K}{4} (V_{xx}^P - V_{yy}^P) \{ (3I_z^2 - I^2) [\sin^2\theta \cos 2\phi + \sin 2\Theta (\frac{1}{2} \sin 2\theta \cos\phi \cos\psi + \sin\theta \sin 2\phi \sin\psi) - \sin^2\Theta (\frac{1}{2} (1 + \cos^2\theta) \cos 2\phi \cos 2\psi + \cos\theta \sin 2\phi \sin 2\psi)] + (I_z I_+ + I_+ I_z) [\frac{3}{2} \sin 2\Theta \sin^2\theta \cos 2\phi + 2 \cos 2\Theta (\sin\theta \sin 2\phi \sin\psi + \frac{1}{2} \sin 2\theta \cos 2\phi \cos\psi) - 2i \cos\Theta (\frac{1}{2} \sin 2\theta \cos 2\phi \sin\psi - \sin\theta \sin 2\phi \cos\psi) - \sin 2\Theta (\frac{1}{2} (1 + \cos^2\theta) \cos 2\phi \cos 2\psi + \cos\theta \sin 2\phi \sin 2\psi) + 2i \sin\Theta (\frac{1}{2} (1 + \cos^2\theta) \cos 2\phi \sin 2\psi - \cos\theta \sin 2\phi \cos 2\psi)] + I_+^2 [-\frac{3}{2} \sin^2\Theta \sin^2\theta \cos 2\phi + 2i \sin\Theta (\frac{1}{2} \sin 2\theta \cos 2\phi \sin\psi - \sin\theta \sin 2\phi \cos\psi) - \sin 2\Theta (\sin\theta \sin 2\phi \sin\psi + \frac{1}{2} \sin 2\theta \cos 2\phi \cos\psi) - (1 + \cos^2\Theta) (\frac{1}{2} (1 + \cos^2\theta) \cos 2\phi \cos 2\psi + \cos\theta \sin 2\phi \sin 2\psi) + 2i \cos\Theta (\frac{1}{2} (1 + \cos^2\theta) \cos 2\phi \sin 2\psi - \cos\theta \sin 2\phi \cos 2\psi)] + \text{c.c.} \}. \quad (\text{A13})$$

Equation (2) is obtained by setting $\Theta = 0$ in (A13).

¹² H. Goldstein, *Classical Mechanics* (Addison-Wesley Publishing Company, Inc., Reading, Massachusetts, 1950), p. 107.